WILEY

USING e-ANNOTATION TOOLS FOR ELECTRONIC PROOF CORRECTION

Required software to e-Annotate PDFs: Adobe Acrobat Professional or Adobe Reader (version 11 or above). (Note that this document uses screenshots from Adobe Reader DC.)
The latest version of Acrobat Reader can be downloaded for free at: http://get.adobe.com/reader/

Once you have Acrobat Reader open on your computer, click on the Comment tab (right-hand panel or under the Tools menu).

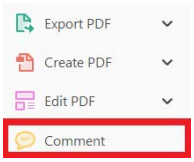

This will open up a ribbon panel at the top of the document. Using a tool will place a comment in the right-hand panel. The tools you will use for annotating your proof are shown below:

1. Replace (Ins) Tool – for replacing text.

Strikes a line through text and opens up a text box where replacement text can be entered.

How to use it:

- Highlight a word or sentence.
- Click on .
- Type the replacement text into the blue box that appears.

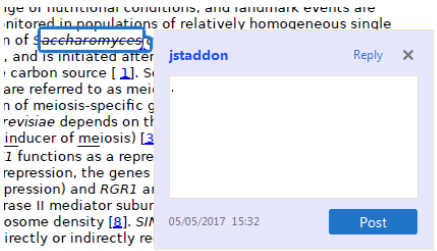

2. Strikethrough (Del) Tool – for deleting text.

Strikes a red line through text that is to be deleted.

How to use it:

- Highlight a word or sentence.
- Click on .
- The text will be struck out in red.

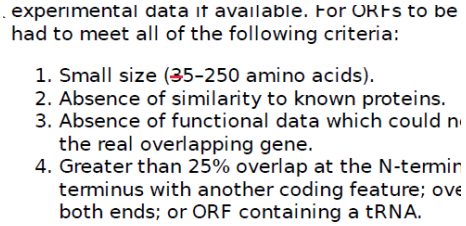

3. Commenting Tool – for highlighting a section to be changed to bold or italic or for general comments.

Use these 2 tools to highlight the text where a comment is then made.

How to use it:

- Click on .
- Click and drag over the text you need to highlight for the comment you will add.
- Click on .
- Click close to the text you just highlighted.
- Type any instructions regarding the text to be altered into the box that appears.

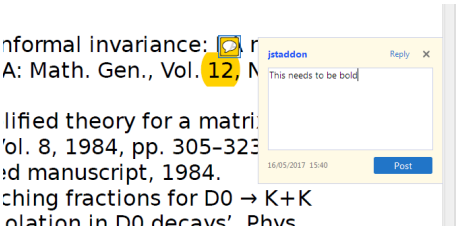

4. Insert Tool – for inserting missing text at specific points in the text.

Marks an insertion point in the text and opens up a text box where comments can be entered.

How to use it:

- Click on .
- Click at the point in the proof where the comment should be inserted.
- Type the comment into the box that appears.

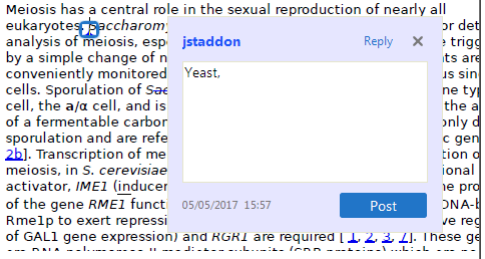

USING e-ANNOTATION TOOLS FOR ELECTRONIC PROOF CORRECTION

5. Attach File Tool – for inserting large amounts of text or replacement figures.

Inserts an icon linking to the attached file in the appropriate place in the text.

How to use it:

- Click on  .
- Click on the proof to where you'd like the attached file to be linked.
- Select the file to be attached from your computer or network.
- Select the colour and type of icon that will appear in the proof. Click OK.

The attachment appears in the right-hand panel.

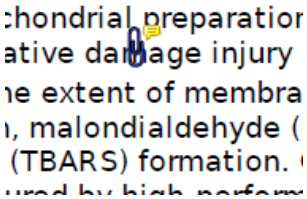

6. Add stamp Tool – for approving a proof if no corrections are required.

Inserts a selected stamp onto an appropriate place in the proof.

How to use it:

- Click on  .
- Select the stamp you want to use. (The Approved stamp is usually available directly in the menu that appears. Others are shown under *Dynamic*, *Sign Here*, *Standard Business*).
- Fill in any details and then click on the proof where you'd like the stamp to appear. (Where a proof is to be approved as it is, this would normally be on the first page).

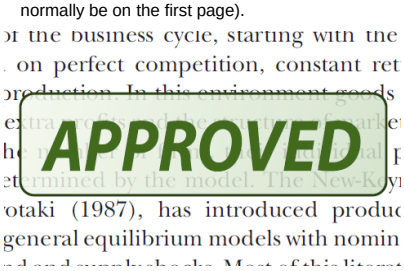

Drawing tools available on comment ribbon

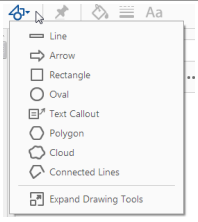

7. Drawing Markups Tools – for drawing shapes, lines, and freeform annotations on proofs and commenting on these marks.

Allows shapes, lines, and freeform annotations to be drawn on proofs and for comments to be made on these marks.

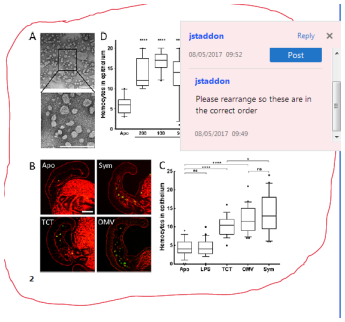

How to use it:

- Click on one of the shapes in the Drawing Markups section.
- Click on the proof at the relevant point and draw the selected shape with the cursor.
- To add a comment to the drawn shape, right-click on shape and select *Open Pop-up Note*.
- Type any text in the red box that appears.

For further information on how to annotate proofs, click on the Help menu to reveal a list of further options:

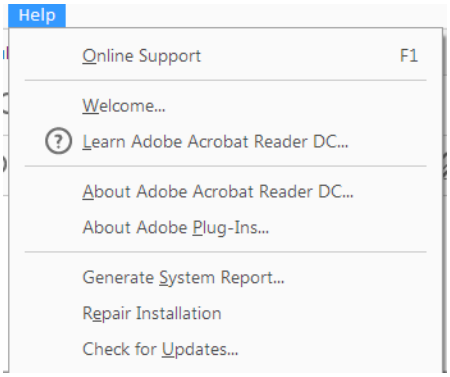

WILEY

Author Query Form

Journal: TPJ

Article: 13732

Dear Author,

During the copyediting of your manuscript the following queries arose.

Please refer to the query reference callout numbers in the page proofs and respond to each by marking the necessary comments using the PDF annotation tools.

Please remember illegible or unclear comments and corrections may delay publication.

Many thanks for your assistance.

Query reference	Query	Remarks
1	**AUTHOR: Please confirm that given names (red) and surnames/family names (green) have been identified correctly.**	
2	**AUTHOR: Please check that authors and their affiliations are correct.**	
3	**AUTHOR: define LET?**	
4	**AUTHOR: Please give address information for Sigma-Aldrich: town, state (if applicable), and country.**	
5	**AUTHOR: Please give address information for Calbiochem: town, state (if applicable), and country.**	

Funding Info Query Form

Please confirm that the funding sponsor list below was correctly extracted from your article: that it includes all funders and that the text has been matched to the correct FundRef Registry organization names. If a name was not found in the FundRef registry, it may not be the canonical name form, it may be a program name rather than an organization name, or it may be an organization not yet included in FundRef Registry. If you know of another name form or a parent organization name for a "not found" item on this list below, please share that information.

FundRef name	FundRef Organization Name (Country)
~~Innovative Training Network~~	Academy of Finland, Finland
~~Solar Energy into Biomass~~	Innovative Training Network (ITN) Solar energy into Biomass (SE2B), European Union
~~Marie Skłodowska-Curie grant~~	University of Turku Doctoral Program in Molecular Life Sciences, Finland

The Plant Journal (2017) doi: 10.1111/tpj.13732

Proteomic characterization of hierarchical megacomplex formation in Arabidopsis thylakoid membrane

Marjaana Rantala, Mikko Tikkanen and Eva-Mari Aro*
Molecular Plant Biology, Department of Biochemistry, University of Turku, Turku FI-20014, Finland

Received 9 August 2017; revised 26 September 2017; accepted 28 September 2017.
*For correspondence (e-mail evaaro@utu.fi).

SUMMARY

Conversion of solar energy into chemical energy in plant chloroplasts concomitantly modifies the thylakoid architecture and hierarchical interactions between pigment–protein complexes. Here, the thylakoids were isolated from light-acclimated Arabidopsis leaves and investigated with respect to the composition of the thylakoid protein complexes and their association into higher molecular mass complexes, the largest one comprising both photosystems (PSII and PSI) and light-harvesting chlorophyll a/b-binding complexes (LHCII). Because the majority of plant light-harvesting capacity is accommodated in LHCII complexes, their structural interaction with photosystem core complexes is extremely important for efficient light harvesting. Specific differences in the strength of LHCII binding to PSII core complexes and the formation of PSII supercomplexes are well characterized. Yet, the role of loosely bound L-LHCII that disconnects to a large extent during the isolation of thylakoid protein complexes remains elusive. Because L-LHCII apparently has a flexible role in light harvesting and energy dissipation, depending on environmental conditions, its close interaction with photosystems is a prerequisite for successful light harvesting *in vivo*. Here, to reveal the labile and fragile light-dependent protein interactions in the thylakoid network, isolated membranes were subjected to sequential solubilization using detergents with differential solubilization capacity and applying strict quality control. Optimized 3D-lpBN-lpBN-sodium dodecyl sulfate–polyacrylamide gel electrophoresis system demonstrated that PSII–LHCII supercomplexes, together with PSI complexes, hierarchically form larger megacomplexes via interactions with L-LHCII trimers. The polypeptide composition of LHCII trimers and the phosphorylation of Lhcb1 and Lhcb2 were examined to determine the light-dependent supramolecular organization of the photosystems into megacomplexes.

Keywords: protein megacomplexes, thylakoid membrane, photosystem, light-harvesting complex, phosphorylation, native gel electrophoresis, 3D-gel electrophoresis, *Arabidopsis thaliana*.

INTRODUCTION

The photosynthetic electron transfer chain in the chloroplast thylakoid membrane is mediated by multisubunit protein complexes, including photosystem (PS) II, cytochrome (Cyt) b_6f and PSI. Both PSII and PSI are associated with peripheral light-harvesting complexes (LHC) that collect photon energy to drive solar energy conversion into chemical energy in reaction centers. PSI is tightly associated with four LHCI antenna subunits, while the dimeric PSII core (C_2) is accompanied by variable amounts of LHCII trimers attached with varying strength to PSII (Boekema *et al.*, 1999; Kouřil *et al.*, 2012). In C_2S_2-complex, one LHCII trimer composed of Lhcb1 and Lhcb2 polypeptides is strongly bound to each PSII core unit via Lhcb5 protein. In the $C_2S_2M_2$-complex, an additional trimer, composed of Lhcb1 and Lhcb3 proteins, is moderately bound to each one of the core monomers via Lhcb4 and Lhcb6 proteins. Furthermore, depending on light conditions, several additional L-LHCII-trimers may loosely associate with the $C_2S_2M_2$-complex (Kouřil *et al.*, 2013). A pool of L-LHCII-trimers may also function as an antenna for PSI under certain light conditions (Caffarri *et al.*, 2009; Wientjes *et al.*, 2013), or energetically connect the entire thylakoid membrane (Wientjes *et al.*, 2013; Benson *et al.*, 2015; Grieco *et al.*, 2015).

The higher plant thylakoid membrane is heterogeneous, comprising both grana stacks and inter-connecting stroma thylakoids. Grana stacking is dependent on the adhesive forces created by cation screening. The formation of strong salt bridges between cations and the stroma-exposed parts of LHCII proteins on adjacent membrane layers are

considered the primary stabilizing force of grana stacking (Murakami and Packer, 1971; Standfuss *et al.*, 2005; Wan *et al.*, 2014), but interactions between the positively charged N-terminus with the negatively charged stromal surface of LHCII also play a role in grana appression (Standfuss *et al.*, 2005). Distinct thylakoid subdomains comprise different compositions of pigment–protein complexes; the appressed grana core mainly consists of PSII–LHCII complexes, while non-appressed stroma thylakoids are enriched in PSI–LHCI complexes and ATPase (Andersson and Anderson, 1980). The protein complex composition in the interface of the grana core and stroma membrane is not as well defined but is enriched in both photosystems (Albertsson, 2001; Suorsa *et al.*, 2015). The lateral distribution of Cyt b_6f between the appressed and non-appressed membranes may occur via adjustments of stromal gap width (Kirchhoff *et al.*, 2017).

During the past decade, with increasing knowledge of regulation of photosynthetic light reactions and with accumulation of experimental data from differentially light-acclimated leaves, the concept of the strict lateral heterogeneity (Andersson and Anderson, 1980) of thylakoid membrane protein complexes has been challenged. Indeed, the previous use of only dark-acclimated plants as experimental material masked the tremendous dynamics in the distribution and interactions of pigment–protein complexes in the thylakoid membrane. Such flexibility is essential to guarantee the balance of excitation energy distribution between PSII and PSI in naturally fluctuating light conditions (Galka *et al.*, 2012; Benson *et al.*, 2015; Grieco *et al.*, 2015; Suorsa *et al.*, 2015). The strictly fine-tuned interactions of thylakoid protein complexes are mediated through redox-regulated and opposing phosphorylation–dephosphorylation of the LHCII trimer polypeptides Lhcb1 and Lhcb2 and PSII core proteins. PSII core proteins D1, D2 and CP47 are reversibly phosphorylated by STN8 kinase and counteracting PBCP phosphatase (Bonardi *et al.*, 2005; Samol *et al.*, 2012), while the corresponding enzymes for reversible LHCII phosphorylation include STN7 kinase (Bellafiore *et al.*, 2005) and TAP38/PPH1 phosphatase (Pribil *et al.*, 2010; Shapiguzov *et al.*, 2010). Reversible phosphorylation of Lhcb2 protein may regulate LHCII attachment to PSI, while Lhcb1 phosphorylation has a role in grana stacking (Pietrzykowska *et al.*, 2014).

Isolation of membrane protein complexes from their native lipid environments involves the use of mild, non-ionic detergents with different properties. The most commonly used detergent, β-dodecyl maltoside (β-DM), releases all protein complexes from the entire thylakoid membrane network (Aro *et al.*, 2005; Järvi *et al.*, 2011), but concomitantly destroys weak hydrophobic interactions between distinct protein complexes (Wittig *et al.*, 2006). Digitonin (DIG) is superior to β-DM in its ability to maintain weak interactions between protein complexes, and is therefore suitable when analyzing labile protein complex networks. However, the analysis of supramolecular networks in the highly heterogeneous thylakoid membrane is not straightforward because the bulky-structured DIG solubilizes protein complexes only from non-appressed regions, leaving the grana core fraction insolubilized (Järvi *et al.*, 2011; Suorsa *et al.*, 2015). Thus, analysis of thylakoid heterogeneity with respect to protein complexes encounters the following dilemma: whether to study the entire thylakoid network at the cost of losing labile protein–protein interactions or whether to analyze labile protein complexes only from non-appressed thylakoid domains (Järvi *et al.*, 2011). Although a vast amount of valuable functional and structural information is available from individual protein complexes, we still miss a holistic understanding of the thylakoid network, where the function of an individual complex is never independent of its environment and interactions with various partners.

Here, by improving the analysis of the heterogeneous thylakoid membrane, we demonstrate the hierarchical formation of the large PSII–LHCII–PSI megacomplex. The interaction and regulation of the amount of PSII and PSI allocated to the megacomplex are differentially regulated via Lhcb1 and Lhcb2 protein phosphorylation.

RESULTS

DIG in aminocaproic acid (ACA) buffer enables gentle solubilization of the entire thylakoid membrane with minimal effects on protein–protein interactions

The heterogeneous organization of the thylakoid membrane, composed of both strongly appressed and non-appressed membranes, is a tremendous challenge for investigation of the labile supramolecular network of pigment–protein complexes. Here, to improve the holistic understanding of labile interactions between the protein complexes in the thylakoid membrane, we demonstrate a new approach for comprehensive and gentle initial isolation of the protein complexes from the entire thylakoid membrane.

The mildest non-ionic detergent, DIG in commonly used bis-tris-HCl (BTH) buffer, releases protein complexes from non-appressed membranes, while a substantial fraction of the membrane remains insolubilized (Järvi *et al.*, 2011). As shown in Figure 1a and b, the commonly used 1% or 2% DIG in BTH buffer only partially solubilized the pigment–protein complexes from the thylakoid membrane, while a large portion of chlorophyll (chl)-containing complexes remained insoluble in the pellet (Figure 1a and b; Table S1). Solubilization of non-appressed membranes is indicated by the chl a/b ratio (4.5 and 3.7 after 1% and 2% DIG/BTH treatments, respectively) that exceeded the overall thylakoid chl a/b ratio (3.0), and conversely by the chl a/b ratios of insolubilized pellets that were lower than the

overall thylakoid chl a/b ratio (2.7 and 2.5, respectively; Figure 1a and b; Table S1). Thus, increasing the DIG concentration from 1% to 2% slightly improved the solubilization but still kept the core of the appressed membranes insolubilized (Figure 1a and b; Table S1). Intriguingly, changing the BTH buffer to ACA buffer resulted in the solubilization of almost the entire thylakoid membrane (more than 90% chl in the solubilized fraction), including appressed grana stacks (Figure 1c; Table S1). Importantly, the chl a/b ratio of the solubilized fraction was 3.0, corresponding to that of the entire thylakoid membrane. This result provided evidence that DIG was equally efficient in solubilizing the non-appressed stroma and appressed grana thylakoid membranes. As a control, the thylakoid membrane was treated with β-DM that, as expected, solubilized 97% of the thylakoids (Figure 1d; Table S1) with a chl a/b ratio of 3.0, similar to that of DIG/ACA. Thus, both the one-step DIG/ACA treatment and β-DM resulted in the solubilization of almost the entire thylakoid membrane without discrimination between different thylakoid domains or pigment–protein complexes.

The next question was whether the thylakoids suspended in ACA preserve the membrane stacking and lateral heterogeneity of the pigment–protein complex distribution. Low-temperature (77K) chl fluorescence measurement is a well-established method to study the energy distribution to PSII and PSI, thus reflecting the structural organization of thylakoid membrane pigment–protein complexes. To study the relative fluorescence emission of PSII and PSI, we diluted the thylakoid suspensions in ACA and BTH buffers, and subsequently recorded their 77K fluorescence emission spectra using fully randomized (–$MgCl_2$) (Murata, 1969) and strictly stacked (+$MgCl_2$) thylakoid membranes as controls. Classical cation depletion experiments (Barber, 1980) have demonstrated the destacking of grana and the consequent randomization of thylakoid membrane pigment–protein complexes, which concomitantly increase excitation energy flow to PSI (Barber, 1980).

As demonstrated in Figure 2a, the 77K fluorescence spectra of intact thylakoids were similar independent of whether the thylakoids were diluted in BTH or ACA buffer, indicating that ACA did not influence the lateral distribution of the pigment–protein complexes along the thylakoid network. In contrast, upon randomization of the thylakoid membrane by $MgCl_2$ depletion, a significant increase in relative fluorescence emission from PSI (peak at 730 nm) at the expense of a decrease in fluorescence emission from PSII (peaks at 685 and 695 nm) indicated a loss of heterogeneity in the lateral distribution of thylakoid protein complexes, resulting in increased excitation energy flow to PSI compared with that to PSII (Figure 2a). Conversely, compared with thylakoids suspended in BTH or ACA, thylakoids suspended in the presence of extra $MgCl_2$ (+$MgCl_2$) exhibited a decrease in energy flow to PSI, as evidenced by the low relative fluorescence from PSI (Figure 2a).

The special characteristic of ACA to allow DIG solubilization of appressed grana membranes (Figure 1c) without randomization of membrane protein complexes (Figure 2a) indicates that ACA allows DIG to enter the tightly appressed grana partitions, through an unknown mechanism (Figure 2b). It is crucial that the composition and protein–protein interactions in the thylakoid membrane remained fairly intact upon ACA treatment, as the randomization of the protein complexes, as in the case of $MgCl_2$ depletion, would not provide a reliable basis for implementing the obtained data.

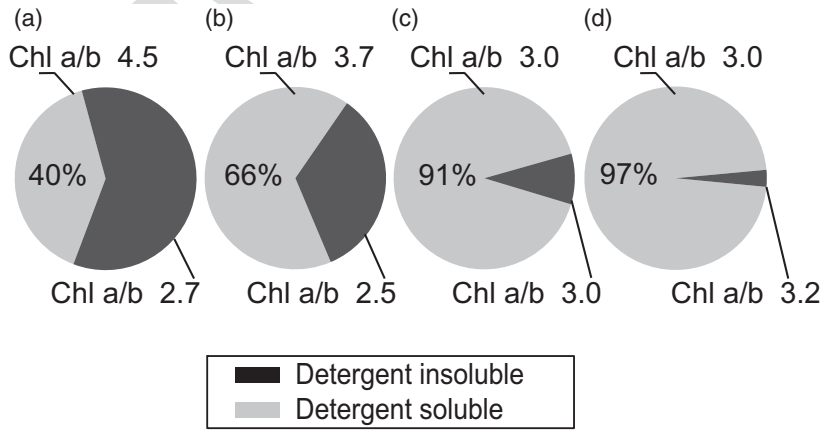

Figure 1. Solubilization of thylakoid pigment–protein complexes with different detergent treatments.
Thylakoid membranes were solubilized with (a) 1% digitonin (DIG) in bis-tris-HCl (BTH) buffer, (b) 2% DIG in BTH buffer, (c) 2% DIG in aminocaproic acid (ACA) buffer or (d) 1% β-dodecyl maltoside (β-DM) in BTH buffer. The insolubilized membranes were pelleted by centrifugation, and the chl content and a/b ratio in the solubilized fraction (supernatant) and insolubilized fraction (pellet) were determined. The chl concentration and chl a/b ratio were measured from three biological replicates.

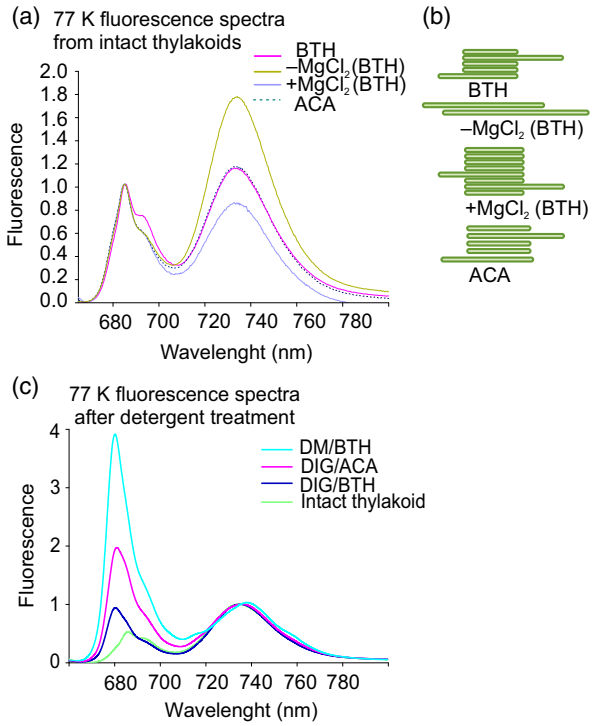

Figure 2. 77K fluorescence emission spectra from intact and detergent-treated thylakoids.
(a) Fluorescence emission at 77K was recorded from intact thylakoid samples diluted in bis-tris-HCl (BTH) buffer and aminocaproic acid (ACA) buffer, as well as from samples with artificially destacked and randomized (–$MgCl_2$) or excessively stacked (+5 mM $MgCl_2$) grana membranes. The 77K fluorescence spectra were recorded at a chl concentration of 3 μg per 100 μL and normalized to F685.
(b) Schematic presentation of the thylakoid architecture as affected by the presence/absence of $MgCl_2$ and the comparison of BTH and ACA buffers.
(c) Fluorescence emission at 77K was recorded from thylakoid samples solubilized with 2% digitonin (DIG)/BTH, 2% DIG/ACA or 1% dodecyl maltoside (DM)/BTH buffer. The fluorescence emission spectra were measured from the solubilized fraction (supernatant) and normalized to the photosystem I (PSI) emission peak. The intact thylakoid membrane (green curve) diluted with BTH buffer was used as a control.

Detergent-specific disconnection of LHCII from the thylakoid membrane integrity

As demonstrated in Figure 2a, and by the green curve in Figure 2c, the 77K fluorescence spectra of intact thylakoid membranes comprise fluorescence emission peaks at 685 nm and 690 nm, which are both derived from PSII, and at 735 nm derived from PSI. Intact or mechanically fractioned thylakoids never reveal a 77K fluorescence emission peak at 680 nm, originating from free LHCII (Andreeva *et al.*, 2003; Tikkanen *et al.*, 2008). In contrast, addition of detergents immediately induced a strong 77K fluorescence emission peak at 680 nm, indicating that a large fraction of LHCII trimers had become energetically uncoupled and thus disconnected from the system (Figure 2c). However, distinct differences exist between the solubilization systems. Even though both DIG/ACA and β-DM treatments resulted in solubilization of the entire thylakoid membrane (Figure 1c and d), there was a significant difference in the emission from uncoupled LHCII trimers between the two detergent treatments. β-DM solubilization resulted in particularly strong relative fluorescence emission at 680 nm (Figure 2c), which is indicative of dissociation of a large fraction of LHCII trimers from the intact thylakoid membrane. Compared with β-DM treatment, DIG/ACA treatment preserved a much larger fraction of LHCII still energetically coupled to photosystems as demonstrated by remarkably lower free-LHCII fluorescence emission at 680 nm (Figure 2c). DIG/BTH solubilization resulted in only partial solubilization of the thylakoid membrane (i.e. the non-appressed domains; Figure 1a), and thus cannot be directly compared with the results obtained with β-DM and DIG/ACA treatments, which do not show discrimination in solubilization of the different thylakoid domains (grana stacks versus non-appressed stroma thylakoids and the margins).

Next, we tested the influence of the release of LHCII with DIG/BTH, DIG/ACA and β-DM treatments on the level of protein complexes by subjecting thylakoids to two-dimensional (2D)-lpBN-sodium dodecyl sulfate–polyacrylamide gel electrophoresis (SDS–PAGE). As shown in Figure 3a, the protein complex patterns of DIG/BTH- and DIG/ACA-treated samples in one-dimensional (1D)-lpBN-PAGE were qualitatively similar, whereas β-DM treatment produced a different pattern of protein complexes. All three thylakoid treatments with detergents resulted in the release of a pool of 'free' LHCII (Figure 3a); here, this pool is denoted as loosely bound L-LHCII as it appeared to be the most easily detachable and detergent-sensitive LHCII structure. DIG/ACA and β-DM treatments also disconnected a fraction of larger LHCII structure, comprised of the LHCII trimer together with Lhcb4 and Lhcb6 proteins (Figure 3a). This LHCII represents disconnected M-LHCII (Caffarri *et al.*, 2009).

Closer inspection of the thylakoid protein complexes in Figure 3a by 2D-SDS–PAGE revealed the individual protein composition of each complex (Figures 3b–d and S1) and allowed for the assignment of the nomenclature of various complexes in Figure 3a. The identification of the protein spots is based on our previous mass spectrometry analyses (Aro *et al.*, 2005; Järvi *et al.*, 2011; Suorsa *et al.*, 2015). Comparison of the SDS–PAGE gels in Figure 3b–d demonstrated several differences between the treatments. (i) Compared with DIG/BTH-treated samples, DIG/ACA-treated samples, which also included grana core domain complexes, had a much higher abundance of PSII complexes. (ii) Upon treatment with DIG/ACA, a large fraction of PSI and almost all PSII complexes was associated with high molecular mass super/megacomplexes (Figure 3c). (iii) The yield of the largest megacomplex (B1) was more pronounced with DIG/ACA treatment than with DIG/BTH treatment. (iv) β-DM solubilization produced smaller complexes

COLOR

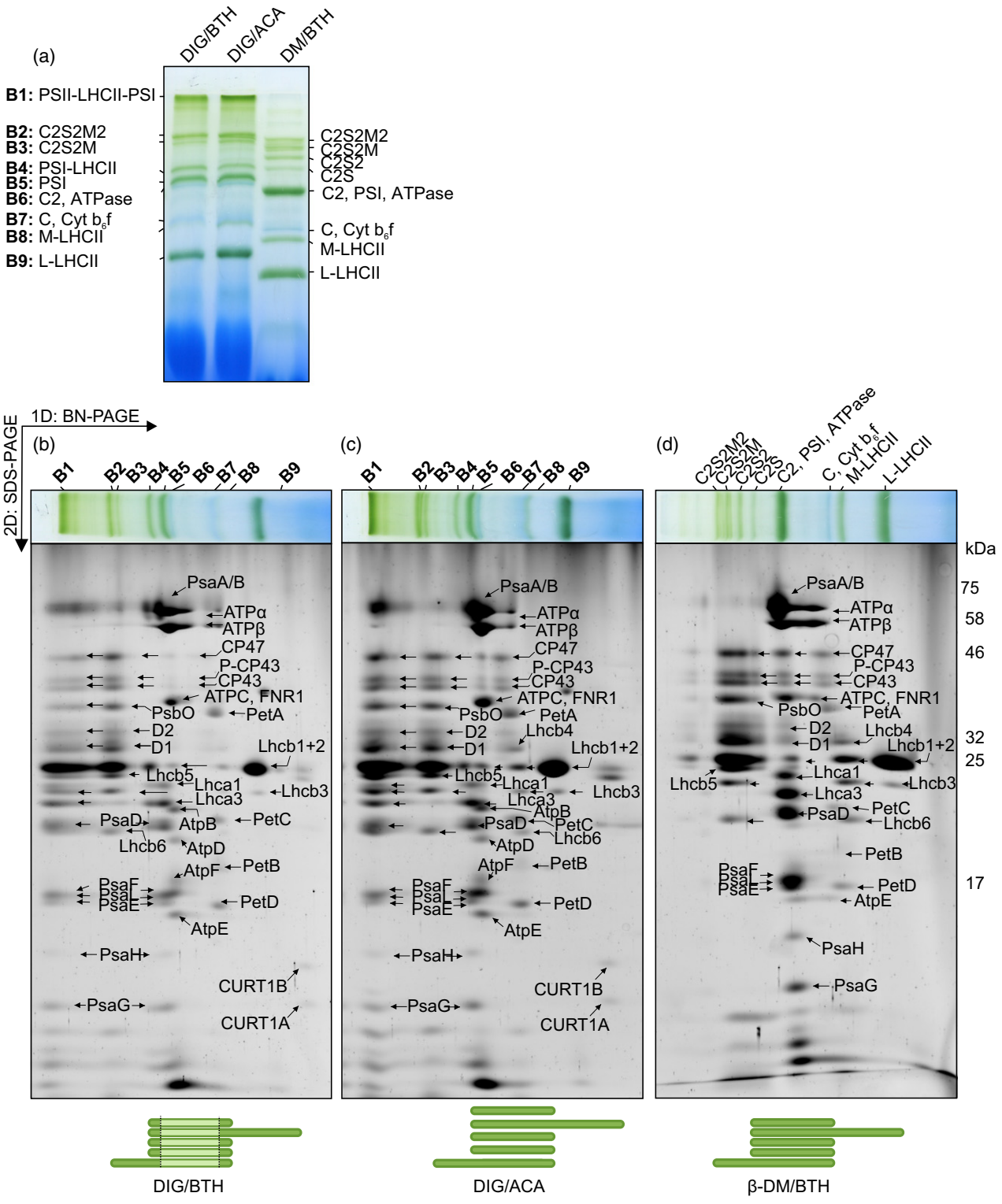

Figure 3. Comparison of the thylakoid membrane protein complexes obtained with different detergent treatments.
(a) Thylakoid membranes solubilized with different detergents were separated on 1D-lpBN-polyacrylamide gel electrophoresis (PAGE). The gel was then sliced and subjected to 2D-sodium dodecyl sulfate (SDS)–PAGE to demonstrate the individual protein composition of each complex. The protein compositions of (b) 2% digitonin (DIG)/bis-tris-HCl (BTH)-, (c) 2% DIG/aminocaproic acid (ACA)- and (d) 1% β-dodecyl maltoside (β-DM)/BTH-treated thylakoids were visualized with SYPRO staining. The dark-green color in the thylakoid membrane illustrations below the 2D-SDS gels demonstrates the region of the thylakoid membrane solubilized by each detergent and used for the analysis. The identification of individual proteins is based on Aro *et al.* (2005), Järvi *et al.* (2011) and Suorsa *et al.* (2015).

(Figure 3d), clearly being unable to preserve the detergent-sensitive interaction between the protein complexes. Thus, β-DM disconnected the individual building blocks of the supramolecular thylakoid network, while DIG/ACA preserved a much more intact system.

Comparison of the 77K fluorescence spectra (Figure 2c) with the composition of protein complexes obtained with different solubilization systems (Figure 3a–d) demonstrated that the capability of DIG to maintain larger supramolecular protein complexes is due to its ability to maintain more interconnected LHCII, including both M-LHCII and L-LHCII, in the system. For further characterization of complexes B1–B9, see below.

Characterization of the large thylakoid mega- and supercomplexes

The DIG/ACA-solubilized thylakoid membrane (Figure 3a, lane DIG/ACA) comprised the largest amount of super- and megacomplexes. To obtain further insights into the composition of these large protein complexes, we used the differential capacity of the detergents to maintain the protein–protein interactions. To this end, the DIG/ACA lane in Figure 3a was treated with 1% β-DM and then subjected to second lpBN-PAGE. As demonstrated in Figure 4, β-DM treatment broke down weak hydrophobic protein–protein interactions, which were not affected by DIG, and thus resulted in dissociation of the large complexes into their subcomplexes during the 2D-lpBN-PAGE. The spots on the diagonal represent protein complexes with preserved masses, whereas the complexes below the diagonal represent dissociated protein subcomplexes (Figure 4; Table S2a). Two intriguing observations were made. First, during 2D-lpBN-PAGE, a large amount of LHCII dissociated from the large protein super- and megacomplexes present in the 1D-lpBN-gel (Figure 4). Second, concomitant with the release of LHCII, the megacomplexes were dissociated into subcomplexes that, by their molecular mass, were identical to those obtained with one-step β-DM solubilization of the entire thylakoid membrane [the control (ctrl) lane on the left in Figure 4 represents direct β-DM solubilization of the entire thylakoid membrane].

To further analyze the composition of each of the DIG/ACA-solubilized protein complexes (B1–B9), the following three-dimensional (3D)-PAGE analysis was performed. First, the 1D-lpBN gel (DIG/ACA lane in Figure 3a) was sliced to collect the bands representing protein complexes B1–B9. The excised bands were treated with β-DM and placed in the well on the top of the second lpBN-PAGE gel. After electrophoresis, nine lanes (corresponding to protein complexes dissociated from complexes B1–B9) were cut out, solubilized with Laemmli buffer and placed horizontally on the top of a SDS–PAGE gel (Figure 5a–i) for 3D-separation of individual proteins comprising the subcomplexes derived from B1–B9 (Figure 5a–i; Table S2b).

Results obtained from the 2D- and 3D-PAGE analyses of the DIG/ACA-solubilized thylakoid protein complexes revealed the hierarchical assembly of the larger protein complexes from the smaller complexes that were released upon β-DM treatment (Figures 4 and 5a–i; Table S2a and b). The largest protein megacomplex (B1) obtained with DIG/ACA treatment was fractioned into four PSII–LHCII supercomplexes, and into PSI complex, PSII monomer (C), M-LHCII and L-LHCII trimer after the β-DM treatment and subsequent 2D-lpBN-PAGE (Figures 4 and 5a). Notably, the ATPase was completely absent, while a small amount of the Cyt b_6f was detected in B1 (Figure 5a). Only a marginal amount of B1 retained its mass after 2D-lpBN-PAGE, indicating that the largest thylakoid megacomplex is maintained by fragile protein–protein interactions that are mostly destroyed by β-DM. The complexes B2 and B3 dissociated into four and three PSII–LHCII supercomplexes, respectively, and into PSII dimer (C_2), M-LHCII and L-LHCII (trimer) (Figures 4, and 5b and c) after the β-DM treatment. The B2 and B3 bands likely represent large $C_2S_2M_{(2)}$ complexes that due to β-DM-induced gradual release of M-LHCII were dissociated into smaller C_2S_2M, C_2S_2 and C_2S supercomplexes. A small amount of PSI was also detected in B2 and B3; thus, it is conceivable that large PSI supercomplexes co-migrate with the $C_2S_2M_{(2)}$ supercomplex in these bands. The composition of these PSI

COLOR

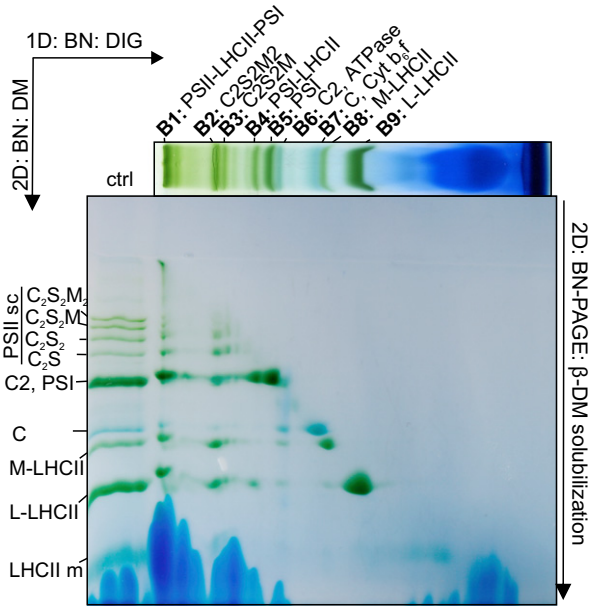

Figure 4. Analysis of the building blocks of the supramolecular protein complex assemblies.
For 2D-lpBN-lpBN-polyacrylamide gel electrophoresis (PAGE), the digitonin (DIG)/aminocaproic acid (ACA)-solubilized protein complexes separated by 1D-lpBN-PAGE (top horizontal lane) were further treated with β-dodecyl maltoside (β-DM) and separated into subcomplexes by 2D-lpBN-PAGE. The ctrl lane on the left represents the thylakoid membranes directly solubilized with β-DM (1D).

COLOR

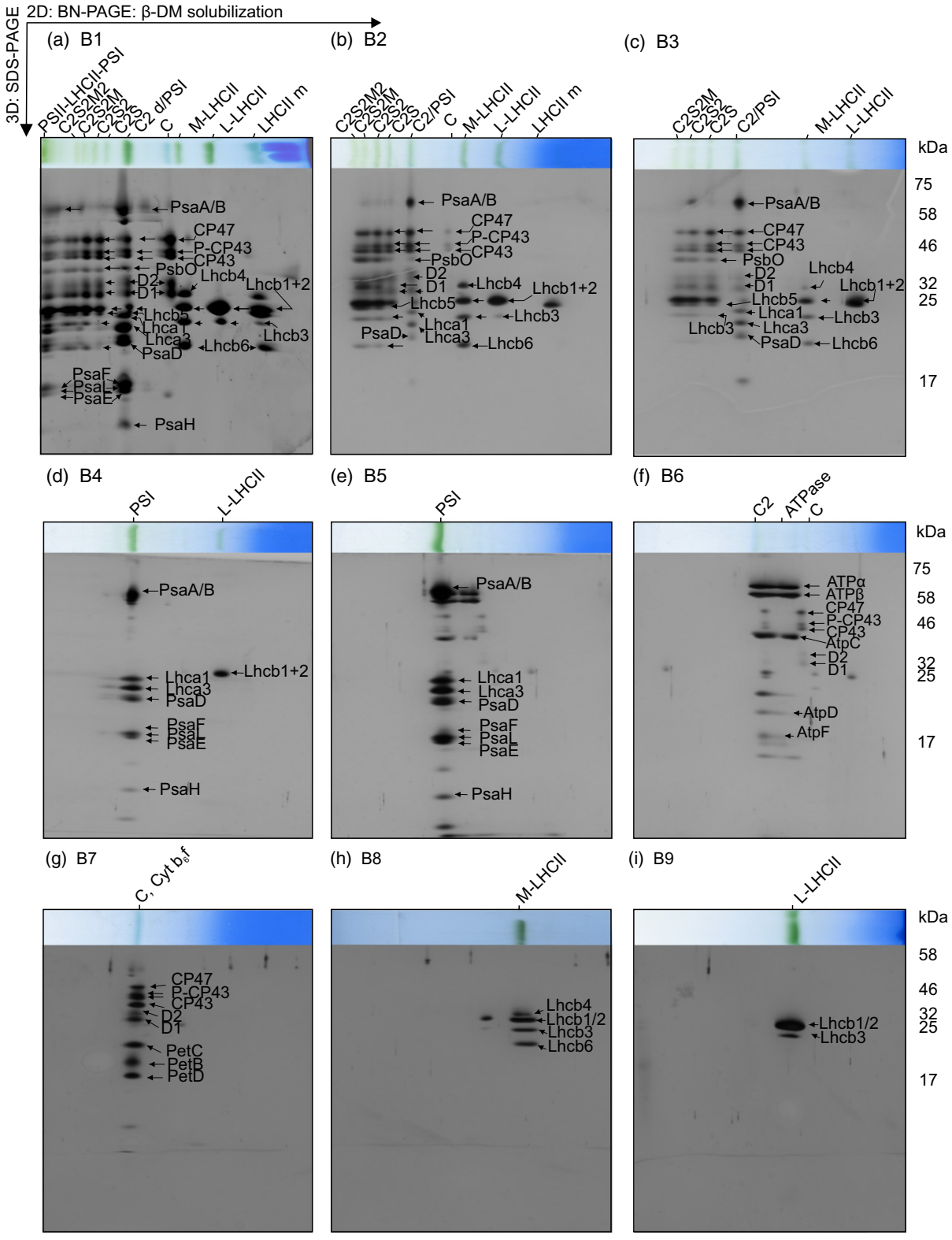

Figure 5. Three-dimensional sodium dodecyl sulfate–polyacrylamide gel electrophoresis (SDS–PAGE) analysis of the original digitonin (DIG)/aminocaproic acid (ACA)-solubilized thylakoid membranes.

The bands representing protein complexes B1–B9 in 1D-lpBN-PAGE were solubilized with β-dodecyl maltoside (β-DM) and run on 2D-lpBN-PAGE gels. The obtained lanes (horizontal gels a–i) were further solubilized with Laemmli buffer, and the protein subunits were separated on 3D-SDS–PAGE gels. The gels were stained with SYPRO Ruby.

megacomplexes remains unknown, but they could represent dimeric or trimeric PSI complexes or monomeric PSI complexes together with several LHCII trimers attached. The B4 band representing PSI–LHCII, 'state-transition' complex was fractioned into PSI and L-LHCII trimer, composed of Lhcb1 and Lhcb2 polypeptides (Figures 4 and 5d) as result of the β-DM treatment. Notably, compared with the amount of LHCII disconnected from complexes B1–B3 and B9, the amount of L-LHCII disconnected from B4 was marginal (Figure 4). The complex B5 (monomeric PSI) retained its integrity after 2D-lpBN-PAGE (Figure 5e), while in B6 the ATPase broke down into smaller ATPase complexes, and a large fraction of PSII dimers broke down into monomers (Figures 4 and 5f). The complexes B7–B9 retained their masses in 2D-lpBN-PAGE (Figure 4) and were further fractioned into their distinct protein subunits in 3D-SDS–PAGE (Figure 5g–i).

Even though both photosystems *in vivo* may form larger mega- and supercomplexes that are preserved only with DIG (complexes B1–B4), both β-DM and DIG/ACA treatments also produced individual PSI monomers, PSII monomers, ATPase and Cyt b_6f, indicating that these complexes are also present independently *in vivo* in the thylakoid membrane.

Distribution of distinct LHCII and P-LHCII proteins in thylakoid super- and megacomplexes

To elucidate the role and origin of the different LHCII structures, 2D-lpBN gels (Figure 4) were subjected to immunoblotting with antibodies raised against Lhcb1, 2 and 3 proteins (Figure 6a–c). As expected, all three Lhcb proteins were found in the PSII supercomplexes released from complexes B1–B3. The M-LHCII released from B1–B3 and B8 comprised Lhcb3 and Lhcb1 proteins, while Lhcb2 was completely absent (Figure 6a–c). The L-LHCII that disconnected from complexes B1–B4 and B9 upon sequential electrophoretic runs was enriched in Lhcb1 and Lhcb2 proteins, but a small amount of Lhcb3 was also detected (Figure 6c). Because Lhcb3 and Lhcb2 do not form homotrimers or any stable complexes together (Pietrzykowska *et al.*, 2014), the free L-LHCII trimers likely represent Lhcb1/Lhcb2 or Lhcb1/Lhcb3 heterotrimers or Lhcb1 homotrimers. The L-LHCII that disconnected from the so-called 'state-transition' complex (B4) was almost exclusively composed of Lhcb1 and Lhcb2, as previously reported (Pietrzykowska *et al.*, 2014; Crepin and Caffarri, 2015).

The Lhcb protein composition and the phosphorylation of the Lhcb1 and Lhcb2 proteins in different complexes were analyzed by immunoblotting of 2D-lpBN gels with P-Lhcb1- and P-Lhcb2-specific antibodies. Intriguingly, in thylakoids isolated from leaves acclimated to steady-state growth light (120 μmol photons m^{-2} sec^{-1}), LHCII was highly phosphorylated at Lhcb1 throughout the PSII–LHCII supercomplexes that were released from B1–B3

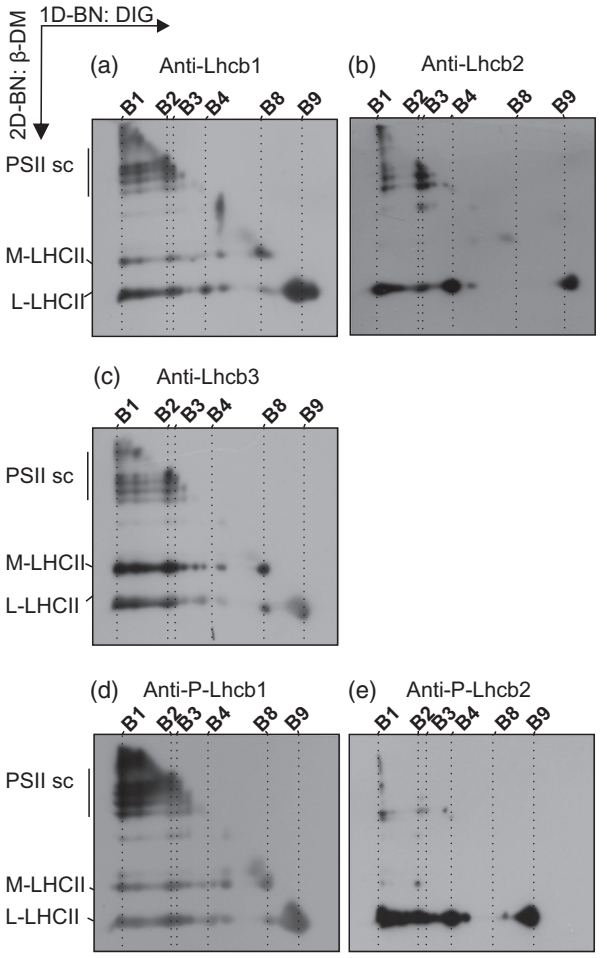

Figure 6. Immunoblots demonstrating the distribution of Lhcb1–3 proteins and P-lhcb1 and -2 proteins in photosystem II (PSII)–light-harvesting chlorophyll a/b-binding complex (LHCII) supercomplexes and disconnected M- and L-LHCII.
The digitonin (DIG)/aminocaproic acid (ACA)-solubilized lane from 1DlpBN-polyacrylamide gel electrophoresis (PAGE) was further solubilized with β-mercaptoethanol and run on 2D-lpBN-PAGE gels. The 2D-lpBN-gel was immunoblotted, and the accumulation of (a) Lhcb1, (b) Lhcb2, (c) Lhcb3, (d) P-Lhcb1 and (e) P-Lhcb2 proteins was detected with specific antibodies.

(Figure 6d). In contrast, Lhcb2 was almost completely dephosphorylated in PSII–LHCII supercomplexes, whereas it was highly phosphorylated in the loosely bound L-LHCIIs that were derived from complexes B1–B4 and B9 (Figure 6e). The disconnected M-LHCII and L-LHCII also contained some phosphorylated Lhcb1 proteins (Figure 6d).

DISCUSSION

Different molecular mechanisms that function in concert to support efficient photosynthesis and protect the photosynthetic apparatus against photodamage in rapidly changing environmental conditions remain poorly characterized (Tikkanen and Aro, 2014; Tiwari *et al.*, 2016). To address these mechanisms, it is crucial to understand the

supramolecular organization of the photosynthetic protein complexes in the thylakoid membrane, as various interactions between the protein complexes are highly dynamic (Suorsa *et al.*, 2015). Achievement of the maximal efficiency of the photosynthetic apparatus in one environmental condition requires a different configuration of thylakoid protein complexes than, for example, that in a condition where protection against photodamage of PSI or PSII is urgently needed. Although the individual thylakoid protein complexes have been thoroughly investigated, the principles of their hierarchical organization and mutual interactions in the entire thylakoid membrane remain surprisingly elusive. Here, we addressed the hierarchical interactions of various thylakoid protein complexes in Arabidopsis plants acclimated to steady-state light conditions that allow balanced function of the photosynthetic apparatus in the thylakoid membrane. Detailed hierarchical analysis of interactions between proteins and protein complexes provides the basis for in-depth analysis of thylakoid membrane dynamics, which are essential for photosynthetic regulation and protection in changing environmental conditions.

Isolation of labile photosynthetic mega- and supercomplexes from heterogeneous thylakoid membranes

To address the question regarding the supramolecular organization of the photosynthetic protein complexes, we developed one-step DIG solubilization of the entire thylakoid membrane. Thus far, the release of the protein complexes from the entire thylakoid membrane has relied on the use of detergents, such as DM or Triton-X, which are unable to maintain weak interactions between protein complexes. In contrast, DIG is considered one of the gentlest detergents to preserve labile protein–protein interactions upon isolation of membrane protein complexes (Schägger and Pfeiffer, 2000), but also has the ability to solubilize only non-appressed membrane domains while leaving grana core domains intact (Järvi *et al.*, 2011). To circumvent this problem, we used an optimized solubilization method in which DIG, in concert with ACA, enables the solubilization of nearly the entire thylakoid membrane, including the appressed grana thylakoids, and concomitantly preserves the labile supramolecular protein–protein interactions (Figures 1c and 3c). Importantly, ACA does not allow randomization of the thylakoid membrane protein complexes as occurs when thylakoids are depleted in divalent cation $MgCl_2$ (−$MgCl_2$; Figure 2a). Instead, ACA facilitates the solubilization of the entire thylakoid membrane by DIG without artificially affecting the distribution of the protein complexes in the thylakoid membrane.

The 77K fluorescence spectra clearly demonstrated that DIG/ACA treatment of the thylakoid membrane preserves notably more L-LHCII attached to the protein complexes than does β-DM treatment (Figure 2c), and accordingly preserves the majority of PSII and a great portion of PSI in large supramolecular structures (Figures 3c, 4 and 7). To resolve the composition of thylakoid mega- and supercomplexes, the DIG/ACA-derived complexes were subjected to β-DM treatment. The treatment resulted in disconnection of the majority of L-LHCII and a fraction of moderately bound M-LHCII from the supramolecular structures (Figures 4 and 7). Concomitant with the release of LHCII, the photosystems that were associated with larger supramolecular structures were released into individual entities (Figures 4 and 5a–d; Table S2a). Therefore, we strongly believe that LHCII *in vivo* determines the hierarchical formation of large supramolecular structures in the thylakoid membrane.

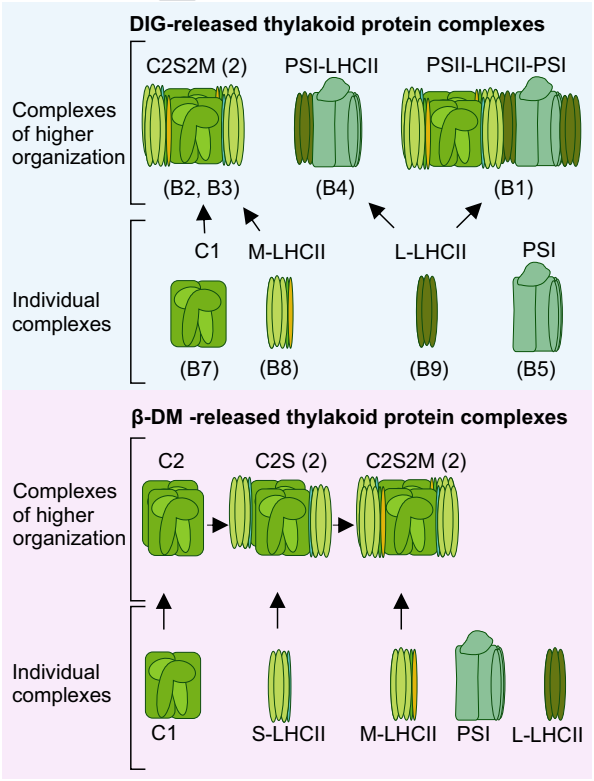

Figure 7. Schematic representation of hierarchical formation of large photosynthetic thylakoid protein complexes from smaller subcomplexes.
Detergent treatment of thylakoid membranes always disconnects part of the light-harvesting chlorophyll a/b-binding complex (LHCII) antennas from the thylakoid membrane integrity. Yet, the digitonin (DIG)/aminocaproic acid (ACA) treatment (upper panel) still preserves a large amount of LHCII interconnected with photosystems. This is indicated by preservation of the labile PSII–LHCII–PSI megacomplexes (B1), large C2S2M(2) supercomplexes (B2, B3) and PSI–LHCII (B4) supercomplexes even after the DIG treatment. A fraction of PSII is present as core monomer (B7), and some M- and L-LHCII (B8 and B9, respectively) are always disconnected from the photosystems. Contrary to the DIG treatment, β-dodecyl maltoside (β-DM) treatment (lower panel) detaches all photosystem-bound L-LHCII, and consequently the labile protein megacomplexes (B1, B4) dissociate during solubilization. β-DM further detaches some of the moderately bound M-LHCIIs from C2S2M2 complexes (B2,B3), thus producing smaller C2S2M and C2S2 supercomplexes.

Hierarchical assembly and putative regulation of thylakoid mega- and supercomplexes

The use of β-DM to release protein subcomplexes from the larger entities, the mega- and supercomplexes obtained by DIG/ACA treatment, not only provided compelling evidence for the existence of specific PSII–PSI megacomplexes in the thylakoid membrane, but also gave a tool to assess the hierarchical assembly of the large thylakoid protein complexes from various protein subcomplexes (Figure 7). As described above, LHCII structures are most important for the formation of larger protein complex assemblies. Based on the strength of LHCII trimer association with the PSII core, the LHCII trimers are classified as strongly bound S-LHCII (comprising Lhcb5 in addition to the LHCII trimer), moderately bound M-LHCII (comprising Lhcb4 and Lhcb6 in addition to the LHCII trimer) and loosely bound L-LHCII trimer (Boekema *et al.*, 1999; Kouřil *et al.*, 2012).

The exact polypeptide composition (Lhcb1–3) of the LHCII trimer determines its interaction with minor antenna (Lhcb4–6) proteins as well as with PSII and PSI. L-LHCII that easily disconnects from the protein mega- and supercomplexes upon sequential solubilization is mainly composed of Lhcb2 and Lhcb1, but some Lhcb3 is also present (Figure 6a–c). Similarly, as expected, all major Lhcb polypeptides are present in the PSII–LHCII supercomplexes derived from complexes B1–B3 by β-DM treatment (Figure 6a–c). Intriguingly, in our study, Lhcb1, but not Lhcb2, is highly phosphorylated throughout the PSII–LHCII supercomplexes (Figure 6d and e), whereas the disconnected L-LHCII trimer is highly phosphorylated at the Lhcb2 polypeptide.

Both Lhcb1 and Lhcb2 are the main substrates for the STN7 kinase (Bellafiore *et al.*, 2005), as well as for the counteracting TAP38/PPH1 phosphatase (Pribil *et al.*, 2010; Shapiguzov *et al.*, 2010), yet the phosphorylation of Lhcb1 and Lhcb2 apparently has distinct and individual roles in the regulation of photosynthesis (Pietrzykowska *et al.*, 2014). A recent report suggests that Lhcb1 phosphorylation affects the flexibility of the appressed membranes (Pietrzykowska *et al.*, 2014) and, here, in accordance, the strong phosphorylation of Lhcb1 in PSII–LHCII supercomplexes (Figure 6d) facilitates the physical interaction of the two photosystems under steady-state illumination. Moreover, strong Lhcb2 phosphorylation in L-LHCII trimers (Figure 6e) is a prerequisite for energy transfer from LHCII to PSI (Pietrzykowska *et al.*, 2014).

Importantly, L-LHCII, which is tightly associated with PSI and disconnects from the PSI–LHCII 'state-transition' complex, clearly represents only a minor fraction of the total L-LHCII associated with the larger mega- and supercomplexes, and detaches from them when β-DM treatment breaks the weak protein–protein interactions (Figure 6d and e). Potentially, the 'state-transition' complex represents only a part of a larger megacomplex that accounts for the energy distribution between PSII and PSI. Indeed, isolated PSI complexes are associated with up to three LHCII trimers rather than just one (Bell *et al.*, 2015; Bos *et al.*, 2017), and it is likely that these larger PSI–LHCII complexes, which may be located in the interphase of grana core and stroma lamella (Bos *et al.*, 2017), have the capacity to also interact with PSII.

Photosystome comprises both pigment–protein complexes involved in LET

Loosely bound L-LHCII, which to a large extent dissociates from larger protein complexes upon β-DM treatment, is associated with both photosystems *in vivo*. Here, we called the isolated PSII–LHCII–PSI megacomplex a photosystome, based on the analogous organization of the respiratory chain protein complexes, the respirasome, in mitochondria (Schägger and Pfeiffer, 2000). The most recent model of the respirasome, a plasticity model, describes the dynamic nature of various associations of the membrane protein complexes (Acìn-Pérez *et al.*, 2008). Similar to the respirasome, the photosystome in the plant thylakoid membrane is speculated to allow fluent and balanced electron transfer between PSII and PSI.

The photosystome is likely located in the interphase of the grana and stroma thylakoids where PSI, with its stroma-protruding structure, can form a large complex with PSII via LHCII. This interaction likely allows the balanced function of the two photosystems. Most importantly, the interactions of the protein complexes forming the photosystome are dynamically regulated by Lhcb1 and Lhcb2 protein phosphorylation, which eventually occurs in concert with many other redox-regulated processes in the thylakoid membrane (Tikkanen and Aro, 2014). We suggest that Lhcb1 phosphorylation in PSII–LHCII mediates the accessibility of PSI to the terminal parts of the grana via regulating the structural flexibility of the membrane (Pietrzykowska *et al.*, 2014). Thus, Lhcb1 phosphorylation ultimately and dynamically regulates the proportion of individual photosystems associated with a photosystome. Moreover, Lhcb2 phosphorylation in the photosystome is essential for excitation energy transfer to PSI from the LHCII antenna system (Pietrzykowska *et al.*, 2014). Although our isolation system excluded the $Cytb_6f$ complex from the photosystome, its presence in the vicinity of the photosystome is likely guaranteed by other concomitantly occurring regulatory mechanisms (Kirchhoff *et al.*, 2017).

EXPERIMENTAL PROCEDURES

Plant material and thylakoid isolation

Arabidopsis thaliana ecotype, Columbia wild-type, was grown under a photon flux density of 120 μmol photons m^{-2} sec^{-1} with an 8-h light/16-h dark regime (GL) at 23°C. OSRAM PowerStar

HQIT 400/D Metal Halide Lamps served as a light source. Leaves from 5-week-old plants were harvested during the light period, 2 h after shifting the lights on, and thylakoids were immediately isolated according to Järvi *et al.* (2011) using buffers supplemented with 10 mM sodium fluoride (NaF). Chlorophyll concentration was determined from the samples according to Porra *et al.* (1989).

Isolation and separation of thylakoid protein complexes

The thylakoid membrane (equivalent to 15 μg of chl) was first pelleted at 6000 ***g*** at 4°C for 2 min, and the supernatant was discarded. The pellet was resuspended in either BTH buffer [25 mM BisTris/HCl (pH 7.0), 20% (w/v) glycerol and 0.25 mg ml^{-1} Pefabloc, 10 mM NaF] or ACA buffer [50 mM BisTris/HCl (pH 7.0), 375 mM ACA, 1 mM EDTA and 0.25 mg ml^{-1} Pefabloc, 10 mM NaF]. An equal volume of detergent solution (in BTH or ACA buffer) was added to the sample to achieve final concentrations of 1% w/v (β-DM; Sigma-Aldrich) and 1% or 2% w/v (DIG; Calbiochem). After solubilization for 2 min on ice (β-DM) or 8 min with continuous gentle mixing (DIG), the insolubilized material was separated by centrifugation at 18 000 ***g*** at 4°C for 20 min. The supernatant was used for the analysis of thylakoid membrane protein complexes. The solubilized thylakoid protein complexes were separated on large-pore (lp) BN-PAGE (as in Järvi *et al.*, 2011), and the composition of complexes was analyzed either with 2D-SDS–PAGE (12% acrylamide, 6 M urea) or 2D-lpBN-lpBN-PAGE (protocol modified from Schägger and Pfeiffer, 2000). For 2D-lpBN-PAGE analysis, the gel slices from 2% DIG/ACA-solubilized protein complexes separated by 1D-lpBN-PAGE were further solubilized with 1% β-DM in BTH for 40 min and subsequently placed horizontally on a second lpBN-PAGE gel to separate the elemental complexes in each band. The 3D-SDS–PAGE analysis from lanes obtained with 2D-lpBN-PAGE was performed in the same manner as 2D-SDS–PAGE, as described in Järvi *et al.* (2011). The proteins were visualized with silver staining (Blum *et al.*, 1987) or SYPRO® Ruby staining according to Invitrogen Molecular Probes™ instructions. For immunological analysis, the 2D-lpBN gels were electroblotted onto polyvinylidene difluoride membranes and immunoprobed with anti-Lhcb1-3 and P-Lhcb1/2 antibodies (Agrisera). Three biological replicates were measured for each experiment.

Randomization of thylakoid membrane and 77K chl a: fluorescence measurements from intact and detergent-treated thylakoids

Thylakoid membranes were diluted with BTH or ACA buffer. To obtain excessively stacked grana membranes, BTH buffer was supplemented with 5 mM $MgCl_2$, while thylakoid randomization and grana destacking were achieved by removing $MgCl_2$ with several washes with BTH buffer (Murata, 1969). Thylakoid membranes were solubilized with different detergents as described above. Fluorescence emission spectra were recorded from intact thylakoids and from the solubilized fractions after detergent treatments (3 μg chl per 100 μL) at 77K with Ocean Optics S2000 spectrometer. Thylakoids were excited with blue light (480 nm wavelength). The signal was normalized to 685 nm (intact thylakoids) or to PSI fluorescence emission peak (detergent-treated thylakoids). Three biological replicates were measured.

ACKNOWLEDGEMENTS

This research was financially supported by the Academy of Finland (project numbers 307335 and 303757), EU-funded Innovative Training Network (ITN) Solar Energy into Biomass (SE2B) Marie Skłodowska-Curie grant agreement (675006) and DPMLS. The authors also thank Virpi Paakkarinen and Ville Käpylä for their excellent technical assistance.

AUTHOR CONTRIBUTIONS

M.R. contributed to designing the experiments, performing the experiments and writing the manuscript; M.T. contributed to designing the experiments and writing the manuscript; E.-M.A. contributed to designing the experiments and was responsible for the final version of the manuscript.

COMPETING FINANCIAL INTERESTS

The authors declare no competing financial interests.

SUPPORTING INFORMATION

Additional Supporting Information may be found in the online version of this article.

Figure S1. Comparison of the thylakoid membrane protein complexes obtained with different detergent treatments.

Table S1 The chl concentration and chl a/b ratio of solubilized and insolubilized thylakoid membrane fractions after detergent treatment

Table S2 (a) The subcomplex composition of the DIG-derived protein complexes B1–B9, and (b) the identified signature proteins of the subcomplexes obtained with β-DM

REFERENCES

Acin-Pérez, R., Fernández-Silva, P., Peleato, M.L., Pérez-Martos, A. and Enriquez, J.A. (2008) Respiratory active mitochondrial supercomplexes. *Mol. Cell*, **32**, 529–539.

Albertsson, P. (2001) A quantitative model of the domain structure of the photosynthetic membrane. *Trends Plant Sci.* **6**, 349–358.

Andersson, B. and Anderson, J.M. (1980) Lateral heterogeneity in the distribution of chlorophyll-protein complexes of the thylakoid membranes of spinach chloroplasts. *Biochim. Biophys. Acta*, **593**, 427–440.

Andreeva, A., Stoitchkova, K., Busheva, M. and Apostolova, E. (2003) Changes in the energy distribution between chlorophyll–protein complexes of thylakoid membranes from pea mutants with modified pigment content: I. Changes due to the modified pigment content. *J. Photochem. Photobiol. B Biol.* **70**, 153–162.

Aro, E.M., Suorsa, M., Rokka, A., Allahverdiyeva, Y., Paakkarinen, V., Saleem, A., Battchikova, N. and Rintamäki, E. (2005) Dynamics of photosystem II: a proteomic approach to thylakoid protein complexes. *J. Exp. Bot.* **56**, 347–356.

Barber, J. (1980) An explanation for the relationship between salt-induced thylakoid stacking and the chlorophyll fluorescence changes associated with changes in spillover of energy from photosystem II to photosystem I. *FEBS Lett.* **118**, 1–10.

Bell, A.J., Frankel, L.K. and Bricker, T.M. (2015) High yield non-detergent isolation of photosystem I-light-harvesting chlorophyll II membranes from spinach thylakoids: implications for the organization of the PSI antennae in higher plants. *J. Biol. Chem.* **290**, 18429–18437.

Bellafiore, S., Barneche, F., Peltier, G. and Rochaix, J.D. (2005) State transitions and light adaptation require chloroplast thylakoid protein kinase STN7. *Nature*, **433**, 892–895.

Benson, S.L., Maheswaran, P., Ware, M.A., Hunter, C.N., Horton, P., Jansson, S., Ruban, A.V. and Johnson, M.P. (2015) An intact light harvesting complex I antenna system is required for complete state transitions in Arabidopsis. *Nat. Plants*, **1**, 15176.

Blum, H., Beier, H. and Gross, H.J. (1987) Improved silver staining of plant proteins, RNA and DNA in polyacrylamide gels. *Electrophoresis*, **8**, 93–99.

Boekema, E.J., van Roon, H., Calkoen, F., Bassi, R. and Dekker, J.P. (1999) Multiple types of association of photosystem II and its light-harvesting antenna in partially solubilized photosystem II membranes. *Biochemistry*, **38**, 2233–2239.

Bonardi, V., Pesaresi, P., Becker, T., Schleiff, E., Wagner, R., Pfannschmidt, T., Jahns, P. and Leister, D. (2005) Photosystem II core phosphorylation and photosynthetic acclimation require two different protein kinases. *Nature*, **437**, 1179–1182.

Bos, I., Bland, K.M., Tian, L., Croce, R., Frankel, L.K., van Amerongen, H., Bricker, T.M. and Wientjes, E. (2017) Multiple LHCII antennae can transfer energy efficiently to a single photosystem I. *Biochim. Biophys. Acta*, **1858**, 371–378.

Caffarri, S., Kouřil, R., Kereiche, S., Boekema, E.J. and Croce, R. (2009) Functional architecture of higher plant photosystem II supercomplexes. *EMBO J.* **28**, 3052–3063.

Crepin, A. and Caffarri, S. (2015) The specific localizations of phosphorylated Lhcb1 and Lhcb2 isoforms reveal the role of Lhcb2 in the formation of the PSI-LHCII supercomplex in arabidopsis during state transitions. *Biochim. Biophys. Acta*, **1847**, 1539–1548.

Galka, P., Santabarbara, S., Khuong, T.T., Degand, H., Morsomme, P., Jennings, R.C., Boekema, E.J. and Caffarri, S. (2012) Functional analyses of the plant photosystem I-light-harvesting complex II supercomplex reveal that light-harvesting complex II loosely bound to photosystem II is a very efficient antenna for photosystem I in state II. *Plant Cell*, **24**, 2963–2978.

Grieco, M., Suorsa, M., Jajoo, A., Tikkanen, M. and Aro, E.M. (2015) Light-harvesting II antenna trimers connect energetically the entire photosynthetic machinery – including both photosystems II and I. *Biochim. Biophys. Acta*, **1847**, 607–619.

Järvi, S., Suorsa, M., Paakkarinen, V. and Aro, E.M. (2011) Optimized native gel systems for separation of thylakoid protein complexes: novel super- and mega-complexes. *Biochem. J.* **439**, 207–214.

Kirchhoff, H., Li, M. and Puthiyaveetil, S. (2017) Sublocalization of cytochrome b 6 f complexes in photosynthetic membranes. *Trends Plant Sci.* **22**, 574–582.

Kouřil, R., Dekker, J.P. and Boekema, E.J. (2012) Supramolecular organization of photosystem II in green plants. *Biochim. Biophys. Acta*, **1817**, 2–12.

Kouřil, R., Wientjes, E., Bultema, J.B., Croce, R. and Boekema, E.J. (2013) High-light vs. low-light: effect of light acclimation on photosystem II composition and organization in *Arabidopsis thaliana*. *Biochim. Biophys. Acta*, **1827**, 411–419.

Murakami, S. and Packer, L. (1971) The role of cations in the organization of chloroplast membranes. *Arch. Biochem. Biophys.* **146**, 337–347.

Murata, N. (1969) Control of excitation transfer in photosynthesis. II. Magnesium ion-dependent distribution of excitation energy between two pigment systems in spinach chloroplasts. *Biochim. Biophys. Acta*, **189**, 171–181.

Pietrzykowska, M., Suorsa, M., Semchonok, D.A., Tikkanen, M., Boekema, E.J., Aro, E.M. and Jansson, S. (2014) The light-harvesting chlorophyll a/b binding proteins Lhcb1 and Lhcb2 play complementary roles during state transitions in *Arabidopsis*. *Plant Cell*, **26**, 3646–3660.

Porra, R.J., Thompson, W.A. and Kriedemann, P.E. (1989) Determination of accurate extinction coefficients and simultaneous equations for assaying chlorophylls a and b extracted with four different solvents: verification of the concentration of chlorophyll standards by atomic absorption spectroscopy. *Biochim. Biophys. Acta*, **975**, 384–394.

Pribil, M., Pesaresi, P., Hertle, A., Barbato, R. and Leister, D. (2010) Role of plastid protein phosphatase TAP38 in LHCII dephosphorylation and thylakoid electron flow. *PLoS Biol.* **8**, e1000288.

Samol, I., Shapiguzov, A., Ingelsson, B., Fucile, G., Crevecoeur, M., Vener, A.V., Rochaix, J.D. and Goldschmidt-Clermont, M. (2012) Identification of a photosystem II phosphatase involved in light acclimation in *Arabidopsis*. *Plant Cell*, **24**, 2596–2609.

Schägger, H. and Pfeiffer, K. (2000) Supercomplexes in the respiratory chains of yeast and mammalian mitochondria. *EMBO J.* **19**, 1777–1783.

Shapiguzov, A., Ingelsson, B., Samol, I., Andres, C., Kessler, F., Rochaix, J.D., Vener, A.V. and Goldschmidt-Clermont, M. (2010) The PPH1 phosphatase is specifically involved in LHCII dephosphorylation and state transitions in Arabidopsis. *Proc. Natl Acad. Sci. USA*, **107**, 4782–4787.

Standfuss, J., Terwisscha van Scheltinga, A.C., Lamborghini, M. and Kuhlbrandt, W. (2005) Mechanisms of photoprotection and nonphotochemical quenching in pea light-harvesting complex at 2.5 A resolution. *EMBO J.* **24**, 919–928.

Suorsa, M., Rantala, M., Mamedov, F., Lespinasse, M., Trotta, A., Grieco, M., Vuorio, E., Tikkanen, M., Järvi, S. and Aro, E.M. (2015) Light acclimation involves dynamic re-organization of the pigment-protein megacomplexes in non-appressed thylakoid domains. *Plant J.* **84**, 360–373.

Tikkanen, M. and Aro, E. (2014) Integrative regulatory network of plant thylakoid energy transduction. *Trends Plant Sci.* **19**, 10–17.

Tikkanen, M., Nurmi, M., Suorsa, M., Danielsson, R., Mamedov, F., Styring, S. and Aro, E.M. (2008) Phosphorylation-dependent regulation of excitation energy distribution between the two photosystems in higher plants. *Biochim. Biophys. Acta*, **1777**, 425–432.

Tiwari, A., Mamedov, F., Grieco, M., Suorsa, M., Jajoo, A., Styring, S., Tikkanen, M. and Aro, E.M. (2016) Photodamage of iron-sulphur clusters in photosystem I induces non-photochemical energy dissipation. *Nat. Plants*, **2**, 16035.

Wan, T., Li, M., Zhao, X., Zhang, J., Liu, Z. and Chang, W. (2014) Crystal structure of a multilayer packed major light-harvesting complex: implications for grana stacking in higher plants. *Mol. Plant.* **7**, 916–919.

Wientjes, E., van Amerongen, H. and Croce, R. (2013) LHCII is an antenna of both photosystems after long-term acclimation. *Biochim. Biophys. Acta*, **1827**, 420–426.

Wittig, I., Braun, H. and Schägger, H. (2006) Blue native PAGE. *Nat. Prot. Elec. Edn*, **1**, 418.